Supplementary Information

TinyPols: a Family of Water-Soluble Binitroxides Tailored for Dynamic Nuclear Polarization Enhanced NMR Spectroscopy at 18.8 and 21.1 T

Alicia Lund, Gilles Casano, Georges Menzildjian, Monu Kaushik, Gabriele Stevanato, Maxim Yulikov, Ribal Jabbour, Dorothea Wisser, Marc Renom-Carrasco, Chloé Thieuleux, Florian Bernada, Hakim Karoui, Didier Siri, Melanie Rosay, Ivan V Sergeyev, David Gajan, Moreno Lelli, Lyndon Emsley, Olivier Ouari, and Anne Lesage

S1 Synthesis details of the series of TinyPol radicals

All chemicals used in synthesis were purchased from Aldrich Chemical Co. Commercially available starting materials were used without further purification. Purification of products was accomplished by flash column chromatography on silica gel (Merck silica gel 60, 230-400mesh) or neutral alumina. Mass spectral analyses were carried out using a Q-STAR Elite at the Aix-Marseille Université Mass Spectrum Facility, Spectropole Saint-Jérôme Marseille. The final products were purified to ≥ 95% and were confirmed by HPLC-MS. HPLC-MS experiments were performed using an Agilent 1260 infinity system coupled with a 6120 simple quadrupole. This system was equipped with a RP C18 column (Zorbax 1.8 μM, 3 x 50 mm) that was equilibrated with 10% vol. MeCN (containing 0.1% (v/v) formic acid) in 0.1% vol. formic acid aqueous solution at the flow rate of 0.28 or 0.40 mL/min. EPR measurements were performed on a BRUKER Elexsys spectrometer operating at 9.4 GHz (X-band) in 50 μL capillaries using the following parameters: microwave power 5 mW and modulation amplitude 0.4 G.

S1.1 Synthesis of TinyPol

Py-TEMPONE **2** was prepared following a procedure reported by Sakai et al [1] and amino nitroxide **9** following a procedure reported by Kubicki et al.[2] The dinitroxide TinyPol was synthesized in a 6-step sequence as shown in Scheme 1. First, 4-cyano Py-TEMPONE (**2**) was prepared in DME using tosyl methyl isocyanide (TOSMIC) in the presence of potassium tert-butoxide adapting a procedure reported by Rauckman et al.[3] Hydrolysis of the cyano group and subsequent reduction of the carboxylic group gave nitroxide **4** in good yield. Oxidation of the hydroxyl group by Dess-Martin periodinane affords nitroxide **5** that is then reacted with amine **9** via a reductive amination reaction using a procedure reported by Sauvée et al.[4] Finally, deprotection of the silyl protected alcohols of **6** by TBAF in THF yields TinyPol as a red solid.
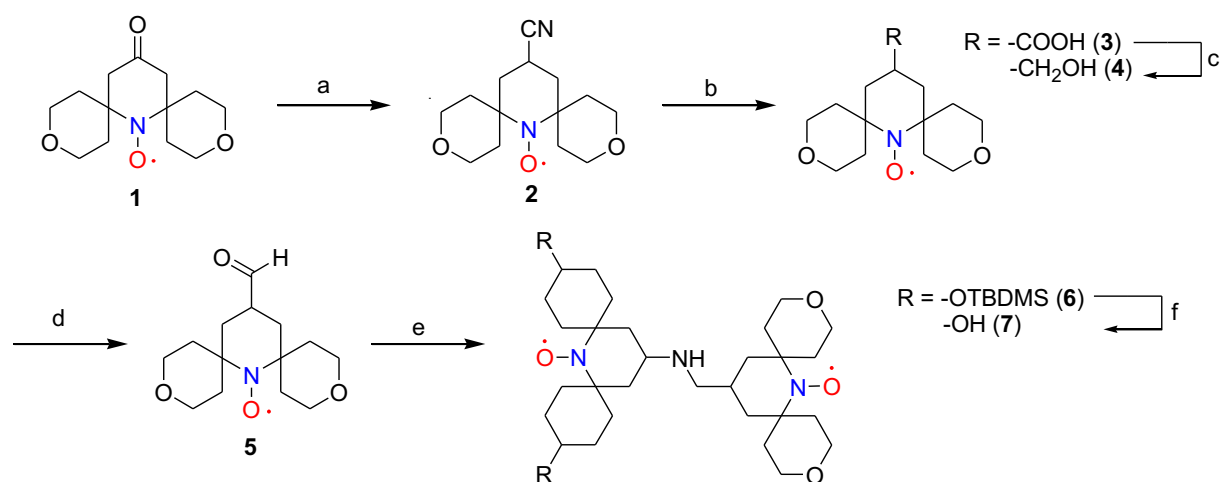
Scheme 1: Synthetic route to TinyPol (7).

Reagents and conditions: (a) TOSMIC, *t*-BuOK, dimethoxyethane, 25°C, 16h. (b) BaH$_2$O$_2$.8H$_2$O, NaOH, MeOH/water, reflux, 16h. (c) BH$_3$ (1M in THF), THF, 25°C, 3h. (d) DMP, DCM, 25°C, 2h. (e) **9**, NaBH(OAc)$_3$, AcOH, THF, 25°C, 16h. (f) TBAF(1M in THF), THF, 25°C, 48h.

Synthesis of compound **2**

To a solution of **1** (1.00 g, 4.00 mmol) and 1-(isocyanomethylsulfonyl)-4-methylbenzene (0.85 g, 4.4 mmol) in 1,2-dimethoxyethane (30 mL) was added dropwise at 0°C a solution of potassium tert-butoxide (0.88 g, 8.00 mmol) and tert-butanol (15 mL) dissolved in 1,2-dimethoxyethane (15 mL). The mixture was stirred at 25°C for overnight. Then, water (150 mL) was added and the solution was extracted with DCM (3 x 80 mL). The organic layer was dried over Na$_2$SO$_4$ and distilled under reduced pressure. The crude product was purified by SiO$_2$ column chromatography using DCM/EtOH (95/5) as eluent to afford compound **2** (0.77 g, 72%) as a pink solid. ESI-MS *m/z*: 266 [M+H]$^+$.

Synthesis of compound **3**

Compound **2** (0.20 g, 0.76 mmol) and barium hydroxide octohydrate (0.95 g, 3.00 mmol) were dissolved in a mixture of water (50 mL) and methanol (25 mL). Then, sodium hydroxide (0.60 g, 15.1 mmol) was added and the mixture was stirred at reflux for 16 h. After cooling, pH was adjusted at 6 with 1N HCl aqueous solution and the mixture was extracted with chloroform (3 x 100 mL). The organic layer was dried over Na$_2$SO$_4$ and distilled under reduced pressure to give compound **3** (0.16 g, 75%). ESI-MS *m/z*: 285 [M+H]$^+$; 307 [M+Na]$^+$

Synthesis of compound **4**

Borane solution (0.80 mL, 1M in THF) was added to a solution of compound **3** (0.22 g, 0.77 mmol) in anhydrous THF (5 mL) at 0°C under argon atmosphere. The reaction mixture was stirred at 25°C for 3 h. After this time, K$_2$CO$_3$ aqueous solution was added to obtain pH = 10. The mixture was extracted with DCM (3 x 50 mL), dried over Na$_2$SO$_4$ and distilled under reduced pressure. The crude product was purified by SiO$_2$ column chromatography using DCM/EtOH (9/1) as eluent to provide compound **4** (0.19 g, 90%) as a pink solid. ESI-MS *m/z*: 271 [M+H]$^+$.

Synthesis of compound **5**

Compound **4** (0.1 g, 0.37 mmol) was dissolved in anhydrous DCM (5 mL) under argon atmosphere. At 0°C, Dess-Martin periodinane (0.19 g, 0.45 mmol) was added in one portion and the reaction mixture was stirred at 25°C for 2 h. After this time, water (15 mL) was added and the mixture was extracted with DCM (3 x 50 mL), dried over Na$_2$SO$_4$ and distilled under reduced pressure. The crude product was purified by SiO$_2$ column chromatography using DCM/EtOH (95/5) as eluent to obtain compound **5** (0.08 g, 80%) as a pink solid. ESI-MS *m/z*: 269 [M+H]$^+$; 291 [M+Na]$^+$

S2

<u>Synthesis of compound **6**</u>

To a stirred solution of compounds **5** (0.08 g, 0.30mmol) in dry THF (2 mL) was added compound **9** (0.16 g, 0.32 mmol) dissolved in dry THF (2 mL) under argon atmosphere. Then, AcOH was added to adjust pH at around 6-7 and the solution was stirred 6 h at 25°C. After this time, NaBH(OAc)$_3$ (0.1 g, 0.458 mmol) was added at 0°C and the solution was stirred at 25°C during 16 h. At the end of reaction, 10 mL of 10% K$_2$CO$_3$ aqueous solution was added. The mixture was extracted with DCM (2 x 50 mL), dried over Na$_2$SO$_4$, concentrated under reduced pressure and the residue was purified by SiO$_2$ column chromatography using DCM/EtOH (99/1) as eluent to provide pure compound **6** (0.11 g, 48%) as a red solid. ESI-MS *m/z*: 765 [M+H]$^+$.

<u>Synthesis of **Tinypol (7)**</u>

A 1 M solution in THF of TBAF (1.5 mL) was added to a stirred solution of compound **6** (0.11 g, 0.14 mmol) in dry THF (3 mL). The solution was stirred 48 h at 25°C. Then, the mixture was concentrated under reduced pressure and the residue was purified by SiO$_2$ column chromatography using DCM/EtOH (100/0 to 80/20) as eluent to provide pure TinyPol

(0.06 g, 80%) as a red solid. HRMS-ESI: m/z calcd. for C$_{29}$H$_{50}$N$_3$O$_6$$^{2\cdot}$ [M+H]$^+$: 536.3694; found 536.3696.
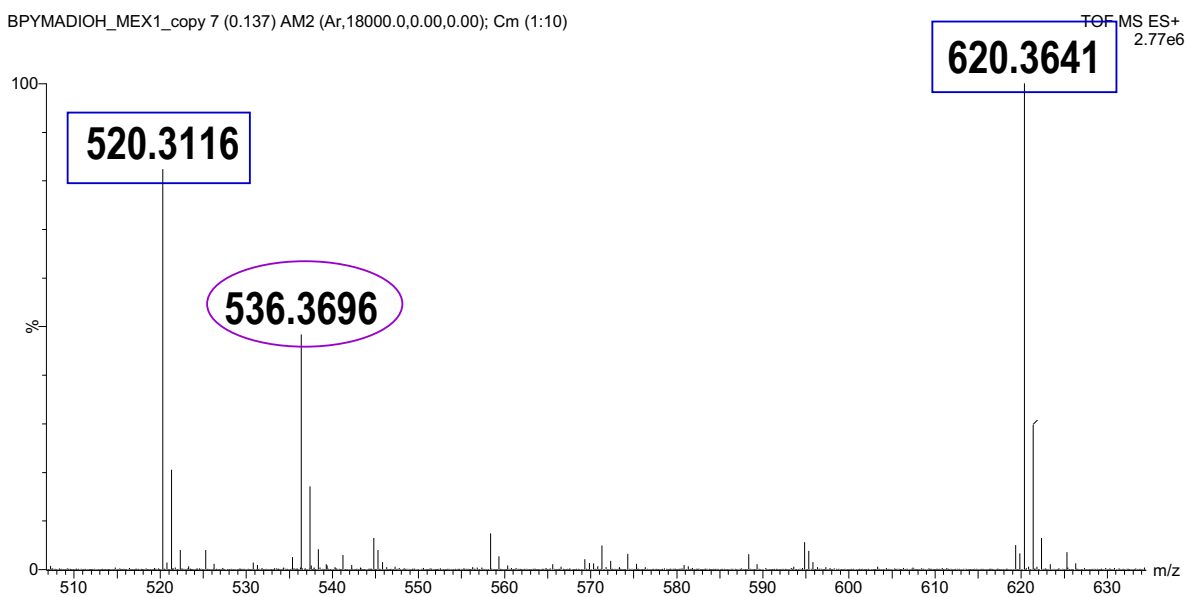
S3

TOF MS ES+
2.77e6

Figure S1: ESI-HRMS spectrum of Tinypol (peaks indicated with blue box correspond to reference peaks for HRMS calibration).
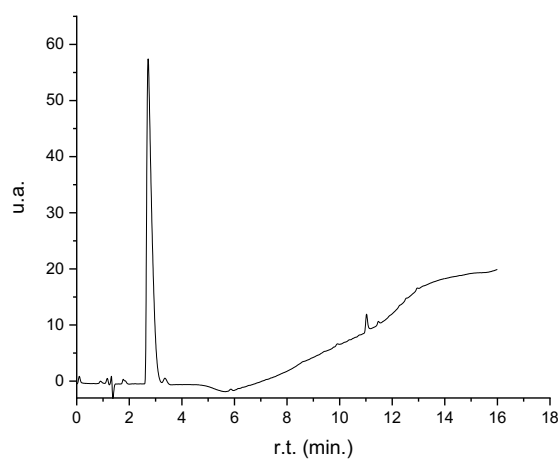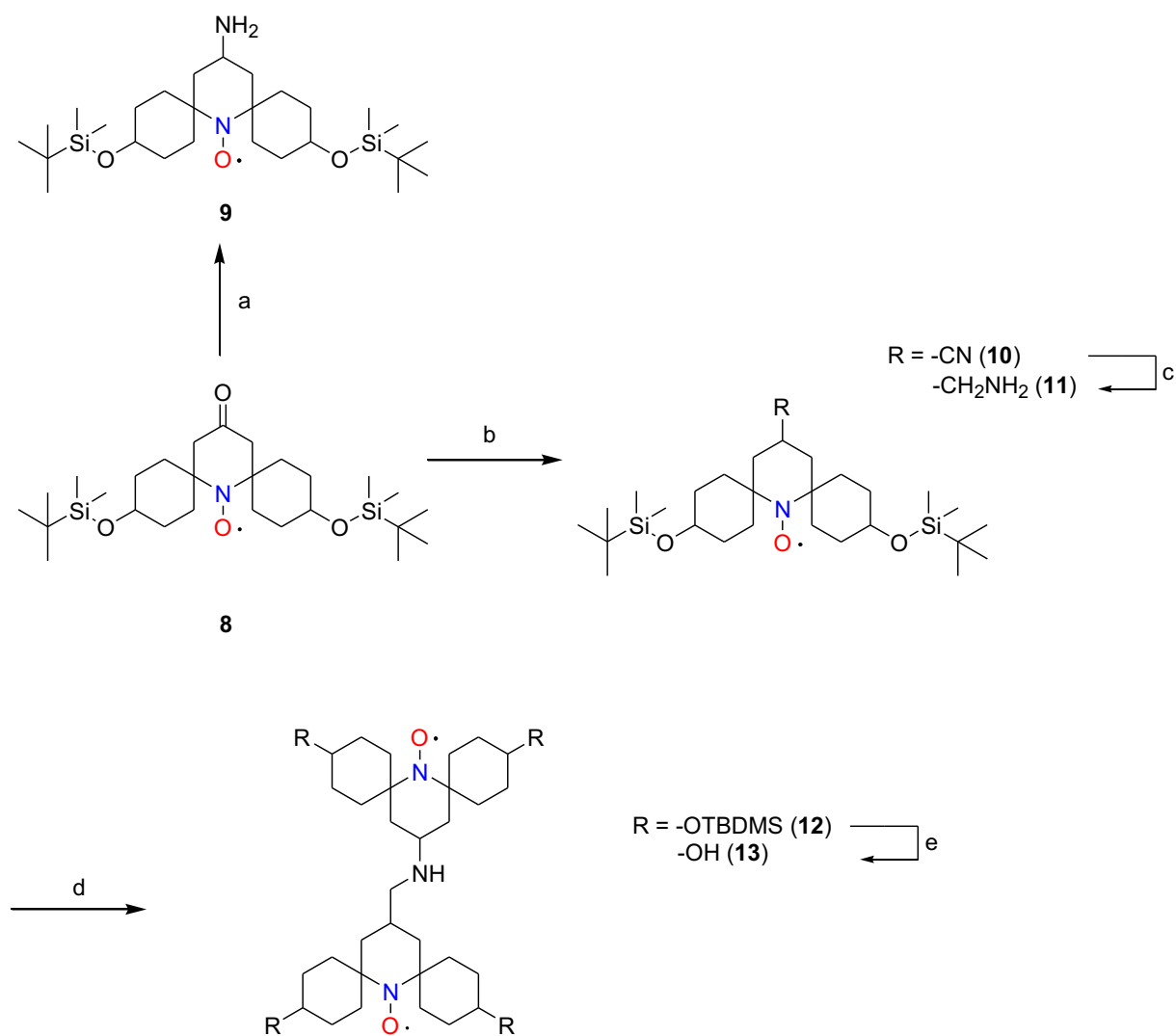

Figure S2: HPLC chromatogram of TinyPol (Water/Acetonitrile/0.1% Formic Acid gradient, RP C18, UV detection at 254 nm)

S4

S1.2 Synthesis of TinyPol-diOH

Scheme 2: Synthetic route to TinyPol-diOH (13)

Reagents and conditions: (a) NH₄OAc, NaBH₃CN, EtOH, 25°C, 24h. (b) TOSMIC, *t*-BuOK, dimethoxyethane, 25°C, 16h. (c) LiAlH₄ (1M in THF), THF anhydrous, 0°C, 3h. (d) **8**, NaBH(OAc)₃, AcOH, THF, 25°C, 16h. (e) TBAF (1M in THF), THF, 25°C, 48h.

<u>Synthesis of compound **9**</u>
Compound **8** (2.0 g, 3.92 mmol) was dissolved in absolute Ethanol (25 mL) under argon atmosphere. Ammonium acetate (3.02 g, 39.2 mmol) was added in one portion. After 6h, NaBH₃CN (0.172 g, 2.73 mmol) was added at 0°C and the solution was stirred at 25°C during 16h. After this time, 10 mL of 10% K₂CO₃ aqueous solution was added. The mixture was extracted with CH₂Cl₂ (2 x 50 mL), dried over Na₂SO₄, concentrated under reduced pressure and the residue was purified by AlO₃ column chromatography using

CH₂Cl₂/EtOH (90/10) as eluent to provide compound **9** (1.20 g, 60%) as a red solid. ESI-MS *m/z*: 512.6 [M+H]⁺

Synthesis of compound **10**

To a solution of **8** (0.56 g, 1.10 mmol) and 1-(isocyanomethylsulfonyl)-4-methylbenzene (0.25 g, 1.28 mmol) in 1,2-dimethoxyethane (10 mL) was added dropwise at 0°C a solution of potassium tert-butoxide (0.25 g, 2.20 mmol) and tert-butanol (5 mL) dissolved in 1,2-dimethoxyethane (5 mL). The mixture was stirred at 25°C for overnight. Then, water (150 mL) was added and the solution was extracted with DCM (3 x 80 mL). The organic layer was dried over Na₂SO₄ and distilled under reduced pressure. The crude product was purified by SiO₂ column chromatography using Pentane/AcOEt (9/1 to 7/3) as eluent to afford compound **10** (0.28 g, 49%) as a pink solid. ESI-MS *m/z*: 522.4 [M+H]⁺; 544.3 [M+Na]⁺.

Synthesis of compound **11**

To a stirred solution of compound **10** (0.06 g, 0.11 mmol) in dry THF (2 mL), LAH (130 µL, 1M in THF) was added slowly at 0°C under argon atmosphere. After 3h à 0°C, the solution was quenched by AcOEt, EtOH and water (5 mL). The mixture was extracted with AcOEt (2 x 20 mL), dried over Na₂SO₄, concentrated under reduced pressure and the residue was purified by neutral alumina column chromatography using DCM/EtOH (99/1 to 90/10) as eluent to give compound **11** (0.03g, 52%) as red solid. ESI-MS *m/z*: 526.4 [M+H]⁺; 548.4 [M+Na]⁺.

Synthesis of compound **12**

To a stirred solution of compounds **11** (0.03 g, 0.057mmol) in dry THF (2 mL) was added compound **8** (0.025 g, 0.05 mmol) dissolved in dry THF (2 mL) under argon atmosphere. Then, AcOH was added to adjust pH at around 6-7 and the solution was stirred 6 h at 25°C. After this time, NaBH(OAc)₃ (0.022 g, 0.104 mmol) was added at 0°C and the solution was stirred at 25°C during 16 h. At the end of reaction, 10 mL of 10% K₂CO₃ aqueous solution was added. The mixture was extracted with DCM (2 x 50 mL), dried over Na₂SO₄, concentrated under reduced pressure and the residue was purified by SiO₂ column chromatography using Pentane/AcOEt (7/3) as eluent to provide pure compound **12** (18.0 mg, 35%) as a red solid. HRMS-ESI: calcd. for C₅₅H₁₁₀N₃O₆Si₄²· ([M+H]⁺) 1020.7466 found 1020.7448.

Synthesis of Tinypol-diOH (**13**)

A 1 M solution in THF of TBAF (1.0 mL) was added to a stirred solution of compound **12** (18.0 mg, 0.017 mmol) in dry THF (2 mL). The solution was stirred 48 h at 25°C. Then, the mixture was concentrated under reduced pressure and the residue was purified by SiO₂ column chromatography using DCM/MeOH (100/0 to 85/15) as eluent to provide pure Tinypol-DiOH (7.00 mg, 73%) as a red solid. HRMS-ESI: calcd. for C₃₁H₅₄N₃O₆²· ([M+H]⁺)564.4007 found 564.4006.
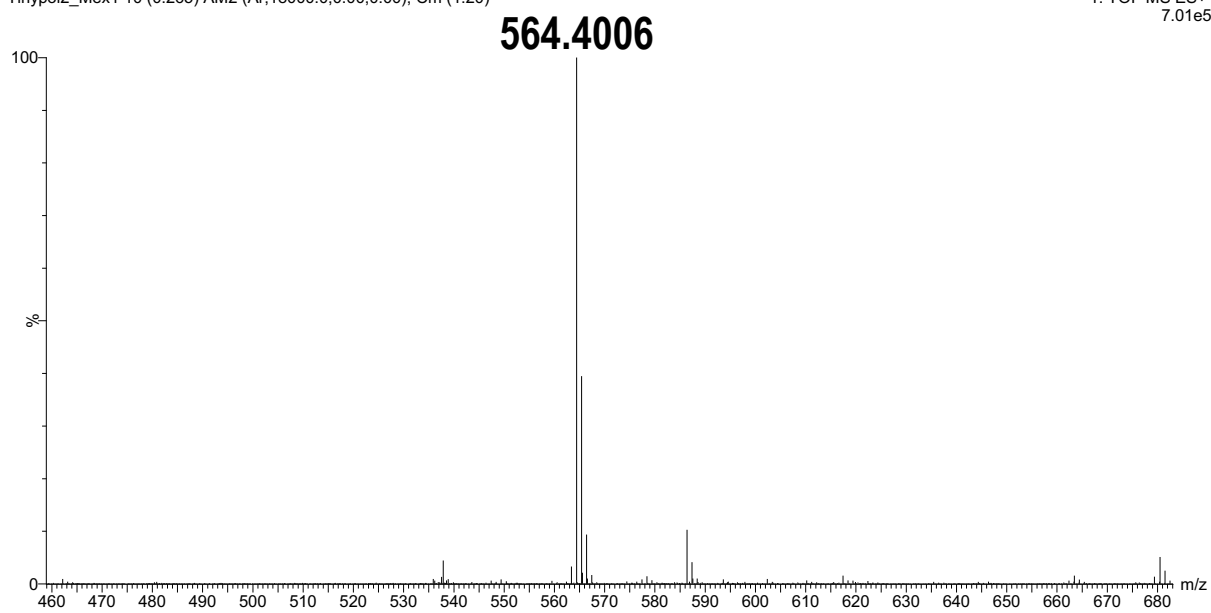
564.4006

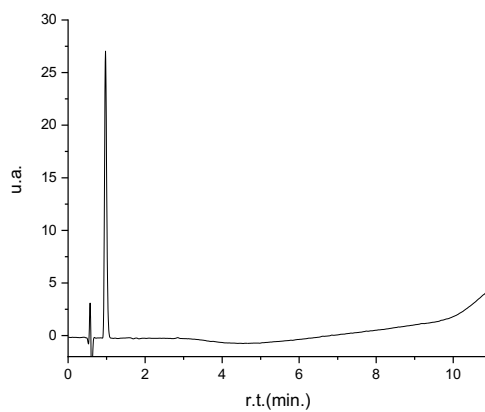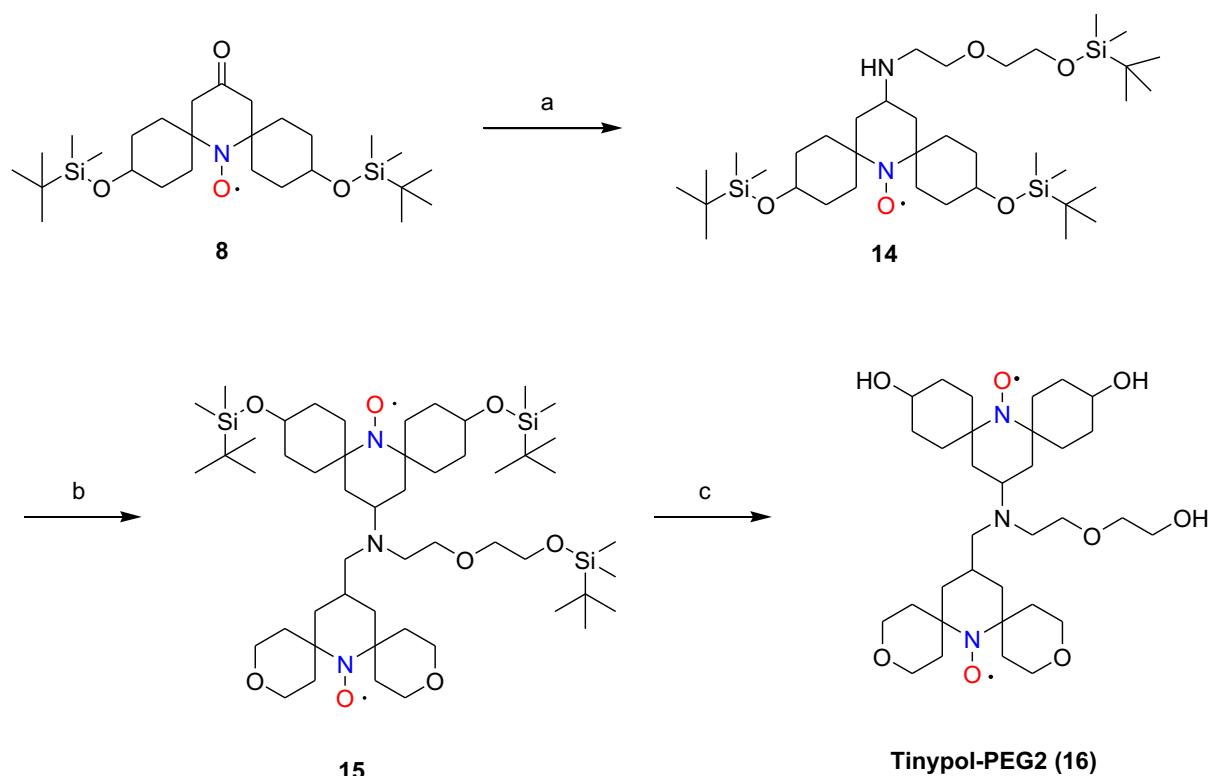**Figure S3**: ESI-HRMS spectrum of **Tinypol-diOH** (**13**)

Figure S4 : HPLC chromatogram of TinyPol-diOH (Water/Acetonitrile/0.1% Formic Acid gradient, RP C18, UV detection at 254 nm)

S1.3 Synthesis of TinyPol-PEG2

Scheme 3: Synthetic route to TinyPol-PEG2 (16)

Reagents and conditions: (a) TBDMS(OCH$_2$CH$_2$)$_2$NH$_2$, NaBH(OAc)$_3$, AcOH, THF, 25°C, 16h. (b) **5**, NaBH(OAc)$_3$, AcOH, THF, 25°C, 16h. (c) TBAF(1M in THF), THF, 25°C, 48h.

Synthesis of compound **14**

To a stirred solution of compounds **8** (0.360 g, 0.70 mmol) in dry THF (10 mL) was added primary amine (0.180 g, 0.82 mmol) under argon atmosphere. Then, AcOH was added to adjust pH at around 6-7 and the solution was stirred 6 h at 25°C. After this time, NaBH(OAc)$_3$ (0.225 g, 1.06 mmol) was added at 0°C and the solution was stirred at 25°C during 16 h. At the end of reaction, 10 mL of 10% K$_2$CO$_3$ aqueous solution was added. The mixture was extracted with CH$_2$Cl$_2$ (2 x 50 mL), dried over Na$_2$SO$_4$, concentrated under reduced pressure and the residue was purified by SiO$_2$ column chromatography using Pentane/AcOEt (100 to 50/50) as eluent to provide compound **14** (0.330 g, 66%) as an orange solid. ESI-MS m/z = 715 [M+H]$^+$;

Synthesis of compound **15**

To a stirred solution of compounds **14** (0.13 g, 0.18mmol) in dry THF (4mL) was added compound **5** (25 mg, 0.15 mmol) dissolved in dry THF (2 mL) under argon atmosphere. Then, AcOH was added to adjust pH at around 6-7 and the solution was stirred 6 h at 25°C.

S8

After this time, NaBH(OAc)$_3$ (50 mg, 0.24 mmol) was added at 0°C and the solution was stirred at 25°C during 16 h. At the end of reaction, 10 mL of 10% K$_2$CO$_3$ aqueous solution was added. The mixture was extracted with DCM (2 x 50 mL), dried over Na$_2$SO$_4$, concentrated under reduced pressure and the residue was purified by SiO$_2$ column chromatography using DCM/EtOH (99/1 to 97/3) as eluent to provide compound **15** (12 mg, 8%) as a red solid. HRMS-ESI: calcd. for C$_{51}$H$_{100}$N$_3$O$_8$Si$_3$$^{2.}$ ([M+H]$^+$) 966.6813 found 966.6783.

Synthesis of Tinypol-PEG2 (**16**)

A 1 M solution in THF of TBAF (0.5 mL) was added to a stirred solution of compound **15** (12.0 mg, 0.012 mmol) in dry THF (2 mL). The solution was stirred 48 h at 25°C. Then, the mixture was concentrated under reduced pressure and the residue was purified by SiO$_2$ column chromatography using DCM/MeOH (100/0 to 90/10) as eluent to provide pure Tinypol-PEG2 (3.0 mg, 40%) as a red solid. HRMS-ESI: calcd. for C$_{33}$H$_{58}$N$_3$O$_8$$^{2.}$ ([M+H]$^+$) 624.4218 found 624.4210 .
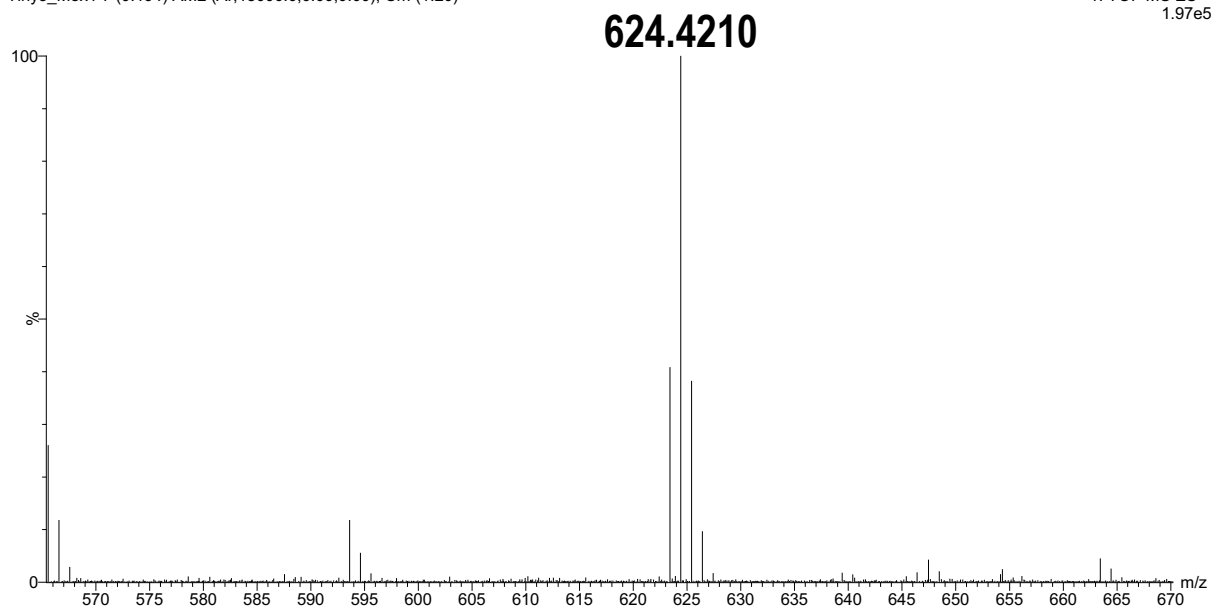
624.4210

Figure S5: ESI-HRMS spectrum of **Tinypol-PEG2 (16)**
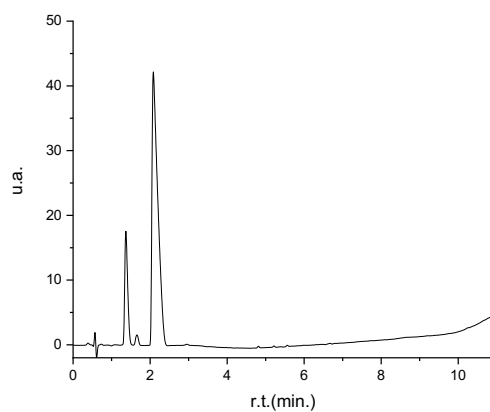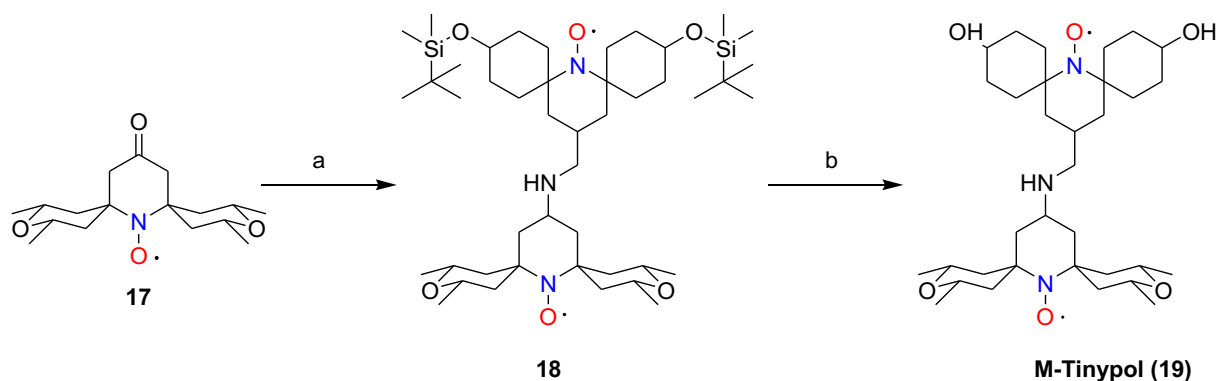

Figure S6 : HPLC chromatogram of TinyPol-PEG2 (Water/Acetonitrile/0.1% Formic Acid gradient, RP C18, UV detection at 254 nm)

S1.4 Synthesis of M-TinyPol

Scheme 4: Synthetic route to M-TinyPol (19)

Reagents and conditions: (a) **11**, NaBH(OAc)₃, AcOH, THF, 25°C, 16h. (b) TBAF(1M in THF), THF, 25°C, 48h.

Synthesis of compound **18**

To a stirred solution of compounds **17** (60.00 mg, 0.19 mmol) in dry THF (3 mL) was added compound **11** (0.12 g, 0.23 mmol) dissolved in dry THF (2 mL) under argon atmosphere. Then, AcOH was added to adjust pH at around 6-7 and the solution was stirred 6 h at 25°C. After this time, NaBH(OAc)₃ (61.00 mg, 0.29 mmol) was added at 0°C and the solution was stirred at 25°C during 16 h. At the end of reaction, 10 mL of 10% K_2CO_3 aqueous solution was added. The mixture was extracted with DCM (2 x 50 mL), dried over Na_2SO_4, concentrated under reduced pressure and the residue was purified by SiO_2 column chromatography using Pentane/AcOEt (7/3) as eluent to provide pure compound **18** (75.00 mg, 48%) as a red solid. ESI-MS *m/z* = 820.6 [M+H]⁺; 842.6 [M+Na]⁺;

Synthesis of M-Tinypol **(19)**

A 1 M solution in THF of TBAF (1.5 mL) was added to a stirred solution of compound **18** (70.00 mg, 0.085 mmol) in dry THF (3 mL). The solution was stirred 48 h at 25°C. Then, the mixture was concentrated under reduced pressure and the residue was purified by SiO_2 column chromatography using DCM/EtOH (100/0 to 90/10) as eluent to provide pure M-Tinypol (25.00 mg, 50%) as a red solid. HRMS-ESI: calcd. for $C_{33}H_{57}N_3O_6^{2.}$ ([M+H]⁺)592.4320 found 592.4320.
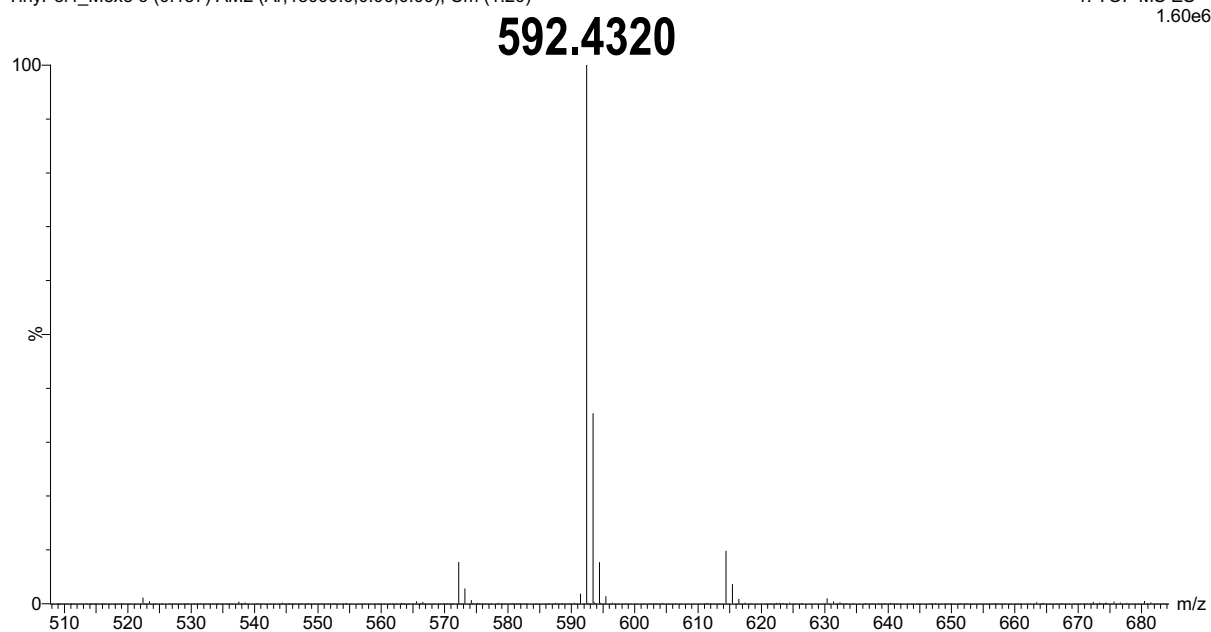
592.4320

Figure S7: ESI-HRMS spectrum of **M-Tinypol** (**19**)
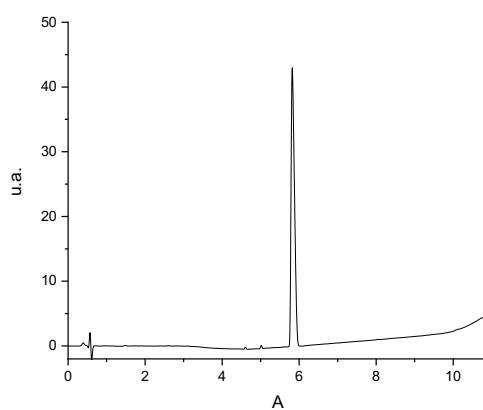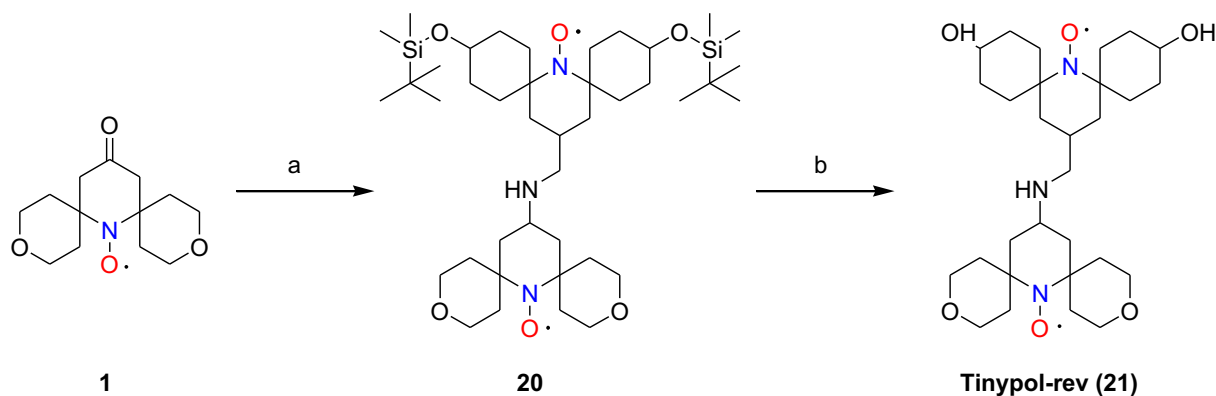

Figure S8: HPLC chromatogram of M-TinyPol (Water/Acetonitrile/0.1% Formic Acid gradient, RP C18, UV detection at 254 nm)

S1.5 Synthesis of TinyPol-rev

Scheme 5: Synthetic route to TinyPol-rev (21)

Reagents and conditions: (a) **11**, NaBH(OAc)$_3$, AcOH, THF, 25°C, 16h. (b) TBAF(1M in THF), THF, 25°C, 48h.

Synthesis of compound **20**

To a stirred solution of compounds **1** (25.0 mg, 0.10 mmol) in dry THF (3 mL) was added compound **11** (60.0 mg, 0.11 mmol) dissolved in dry THF (2 mL) under argon atmosphere. Then, AcOH was added to adjust pH at around 6-7 and the solution was stirred 6 h at 25°C. After this time, NaBH(OAc)$_3$ (32.00 mg, 0.15 mmol) was added at 0°C and the solution was stirred at 25°C during 16 h. At the end of reaction, 10 mL of 10% K$_2$CO$_3$ aqueous solution was added. The mixture was extracted with DCM (2 x 50 mL), dried over Na$_2$SO$_4$, concentrated under reduced pressure and the residue was purified by SiO$_2$ column chromatography using DCM/EtOH (95/5) as eluent to provide pure compound **20** (25.00 mg, 32%) as a red solid. ESI-MS m/z = 764.6 [M+H]$^+$

Synthesis of Tinypol-rev (21)

A 1 M solution in THF of TBAF (0.5 mL) was added to a stirred solution of compound **20** (20.00 mg, 0.026 mmol) in dry THF (3 mL). The solution was stirred 48 h at 25°C. Then, the mixture was concentrated under reduced pressure and the residue was purified by SiO$_2$ column chromatography using DCM/EtOH (100/0 to 85/15) as eluent to provide pure Tinypol-rev (7.00 mg, 50%) as a red solid. HRMS-ESI: calcd. for C$_{29}$H$_{50}$N$_3$O$_6$$^{2.}$ ([M+H]$^+$)536.3694 found 536.3693. ESI-MS m/z = 536.4 [M+H]$^+$
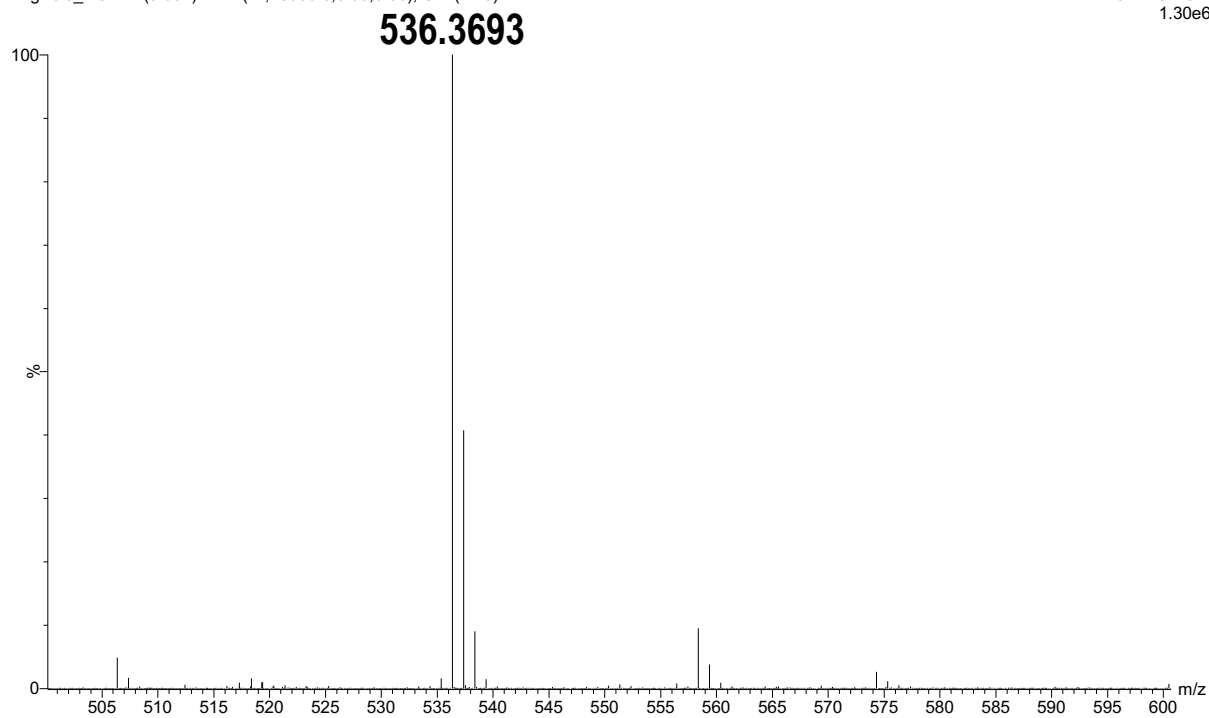
536.3693

Figure S9: ESI-HRMS spectrum of **Tinypol-rev** (**21**)
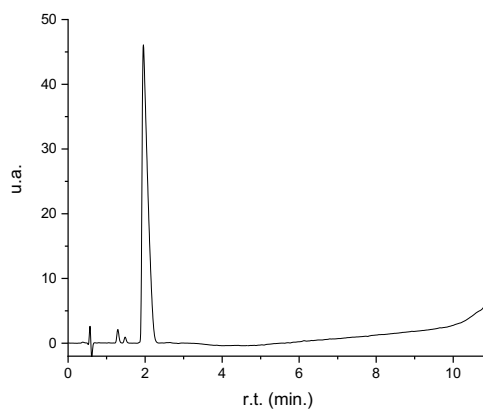

Figure S10 : HPLC chromatogram of TinyPol-rev (Water/Acetonitrile/0.1% Formic Acid gradient, RP C18, UV detection at 254 nm)

S14

S1.6   Structural parameters for TinyPol from Molecular Dynamics

Distance, angle and J values were calculated from 100 ns MD simulations in NVT ensemble carried out at 278 K in water with the Gromacs 2019 package[5] using an AMBER force field (ff99SB)[6] which includes parameters optimized by Barone et al.[7] for the N-O• group. The molecule was embedded into a cubic box containing about 1000 water molecules. We relaxed the volume of the simulation box by performing a NPT simulation of 300 ps duration (278, 1 atm). Once this initial run was achieved, the simulation was then restarted in the NVT ensemble during 100ns. Each conformer was extracted every 1 ns to insure no correlation between the conformers. Singlet and triplet state energies of each conformer were calculated with the Gaussian168 package at a CAM-B3LYP/SVP level of theory. The isotropic J values were calculated applying the Broken Symmetry (BS) formalism on the 100 geometries extracted from MD simulations. The isotropic J values were calculated with the Gaussian16 package[8] at a CAM-B3LYP/SVP level of theory and applying the Broken Symmetry (BS) formalism on 100 geometries extracted from MD simulations. A superfine grid and an energy threshold at 10^{-10} Hartree were used to insure sufficient numerical accuracy in the calculations. The Yamaguchi equation[9] was then used to calculate the J coupling according to:

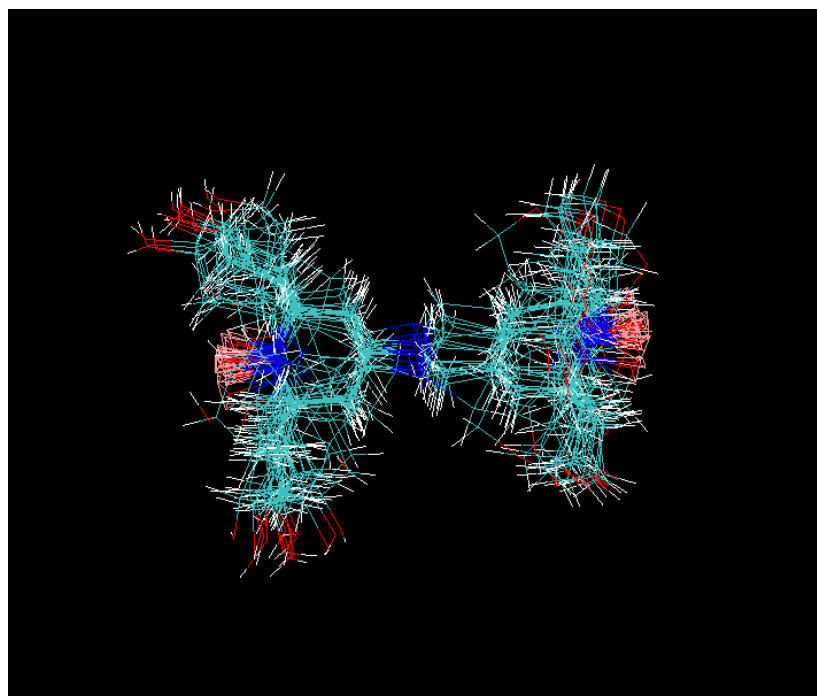$$J = \frac{E_T - E_{BS}}{<\hat{S}^2>_T - <\hat{S}^2>_{BS}}$$

Figure S11: Structural ensembles for TinyPol. The structures of 20 rotamers were refined using geometrical constraints obtained from 100 ns MD simulations in NVT ensemble carried out at 278 K in water with Gromacs 2019 package using the AMBER force field.
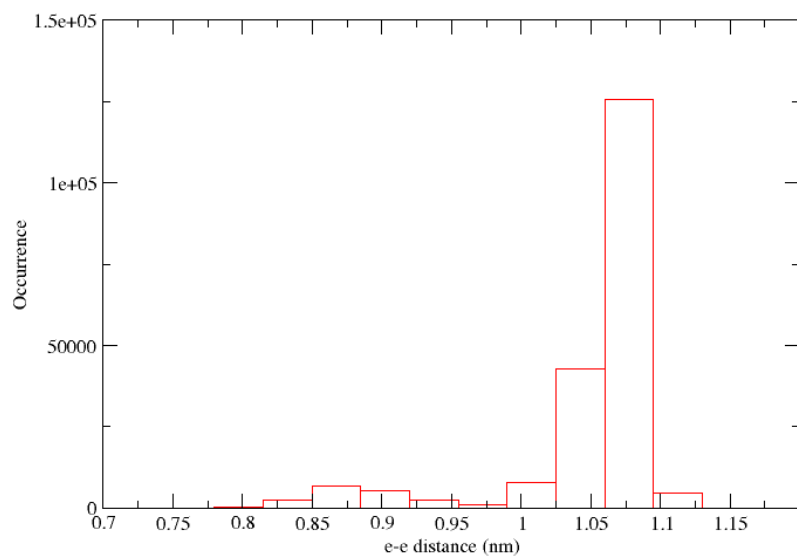
S15

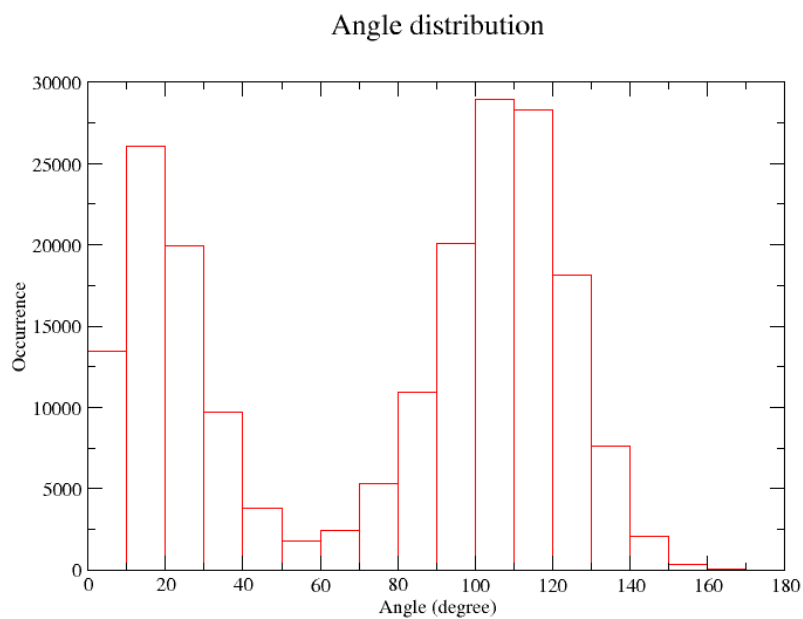**Figure S12:** Distance distribution (in nm) between the two unpaired electrons in TinyPol.

Figure S13: Distribution of angular values (in degrees) in TinyPol between the mean planes of the nitroxide moieties. We note a bimodal distribution with two maxima close to 0° and 90° respectively.
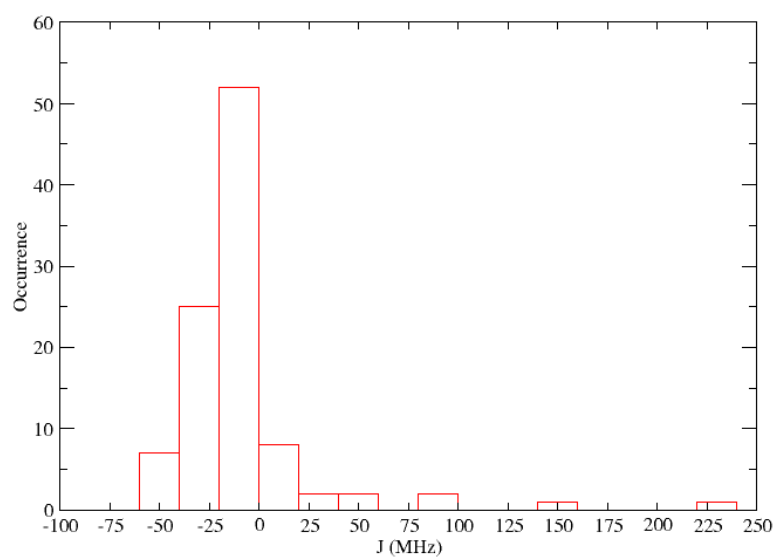
S17

Figure S14: Distribution of isotropic *J* coupling (in MHz) in TinyPol

S2 Sample Preparations

S2.1 Sample preparation for the DNP experiments.

The deuterated solvents glycerol-d$_8$ and D$_2$O, were both purchased from Sigma Aldrich and used without further purification. [13]C,[15]N-labelled proline (Cambridge Isotopes Laboratories), ^{13}C labelled urea and KBr salt (Sigma Aldrich) were also used as received. The studied solutions were prepared by dissolving c.a. 1 mg of the radical powders in d$_8$-glycerol/D$_2$O/H$_2$O 60/30/10 (v/v/v) up to the desired concentration. For measurements at 21.1 T in 3.2 mm rotors, labelled proline at a concentration of 0.2 M (or labelled urea at 2 M for the experiment reported on Fig S27) was added in the solvent matrix to evaluate enhancements from ^{13}C spectra. For AMUPol and M-TinyPol solutions, mechanical stirring at room temperature was sufficient to achieve a radical concentration of up to 20 mM. In contrast, for TinyPol, a maximum concentration of 5 mM could be obtained and required several cycles of sonication for 20 min at 60 °C followed by vortexing for 1 min in order to fully dissolve the radical.

For DNP measurements at both 9.4 T and 18.8 T the solution was then pipetted into a 1.3 mm zirconia rotor that had been pre-packed with a small pellet of ground KBr in order to monitor the temperature via [79]Br T$_1$.[10] For the DNP measurements at 21.1 T the solution was pipetted into a 3.2 mm sapphire rotor, confined with a silicon plug and a zirconia cap. A small pellet of KBr coated by nail polish to prevent the salt from dissolving in the solutions was added to the bottom of the rotor.

S2.1 Synthesis of the material

The inidazolium-containing material and all the intermediates were prepared according to a protocol reported by Romanenko *et al.*[11] with a theoretical ratio imidazolium/Si = 30.

Nitrogen adsorption-desorption isotherm: a$_{S,BET}$: 573 m^2/g, d$_{p,BJH}$: 7nm; Elemental analysis: Si 37,70%, , N 1,03 % (exp.: N/Si = 18; Imidazolium/Si = 36 - theo : N/Si = 15; Imidazolium/Si = 30)
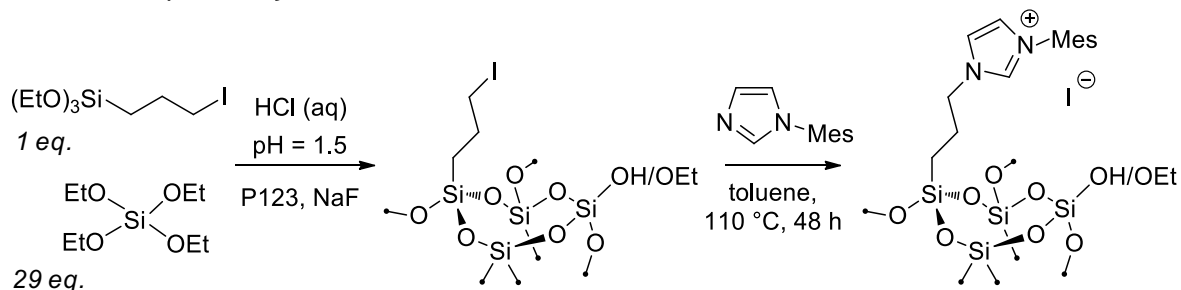
S3 DNP-NMR Methods

MAS DNP NMR experiments were performed on Bruker Avance III wide bore spectrometers, operating at 9.4, 18.8 and 21.1 T, and equipped with triple resonance 1.3 mm (for 9.4 and 18.8 T) and 3.2 mm (for 21.1 T) low-temperature MAS probes. DNP was achieved by irradiating the sample with high-power microwaves at frequencies of 263 GHz (9.4 T) 527 GHz (18.8 T) and 593 GHz (21.1 T) generated by a gyrotron that was operating continuously during the DNP experiments (stability of better than ±1%). A microwave power of 40 W was used at 9.4 T, 22 W at 18.8 T and 9 W at 21.1 T measured at the bottom of the probe. For the experiments at 9.4 and 18.8 T, the field position has been adjusted for optimal cross-effect. At 21.1 T, the gyrotron microwave cavity temperature was optimized to 21.5±0.2 °C. The collector current was also carefully optimized in all cases.

One-dimensional ^{1}H NMR spectra were recorded for all samples at 9.4 T and 18.8 T. The direct excitation experiments were acquired with a DEPTH pulse sequence in order to suppress the background of the probes. The DEPTH sequence consists of a π/2 pulse followed by two π pulses which are phase cycled according to a combined "EXORCYCLE" and "CYCLOPS" scheme.[12-14] The π/2 pulses of 2.5 μs and π of 5 μs (100 kHz RF field) were used. At 18.8 T, the background signal of the probe could not be fully suppressed using DEPTH experiments, and an additional background correction using TopSpin was applied. At 21.1 T, enhancements were measured from the proline signals in ^{13}C one-dimensional CPMAS spectra, as the presence of the silicon plug yields a strong proton signal overlapping with the resonance of the solvent. The DNP enhancement factor was obtained from by taking the ratio of the intensity of the microwave on signal to the intensity of the NMR signal in the absence of microwaves, using a recycle delay of 1.3*$T_{B,ON}$. ^{1}H longitudinal relaxation times (T_1) and DNP build-up times ($T_{B,ON}$) were measured with a standard saturation recovery sequence followed by a rotor synchronized echo period before signal acquisition under microwave off and microwave on conditions respectively. For experiments in 1.3 mm rotors, ^{79}Br T_1 was used to monitor the sample temperature and ensure uniformity (± 2°C) across the spinning speed range, and between microwave on and off experiments. For experiments in 3.2 mm rotors, the temperature was also monitored but could not be maintained at the same value for microwave on and off experiments.

S4 Contribution factor and overall sensitivity gain

The contribution factor for 9.4 T and 18.8 T was measured from 1D ^{1}H spectra by taking the ratio the NMR signal intensity (per unit of mass) of the frozen solution with radical divided by the NMR signal intensity (per unit of mass) of the frozen solution without radical, both measured in the absence of microwave irradiations and with a recycle delay of 5*T_1. The contribution factor was then calculated according to the following equation:

$$\theta = \frac{I_{with\ radical,\mu w\ off}}{I_{without\ radical,\mu w\ off}} \qquad (1)$$

At 21.1 T the contribution factor was calculated from the carbon-13 CPMAS spectra.

The overall sensitivity gain Σ was calculated according to equation 2.

$$\Sigma = \varepsilon \cdot \theta \cdot \sqrt{\frac{T_{B,solvent}}{T_{B,on}}} \qquad (2)$$

where ε is the enhancement factor calculated as the ratio of signal intensity microwave on divided by signal intensity microwave off, θ is the contribution factor defined in equation (1), $T_{B,solvent}$ and $T_{B\ on}$ are the build-up times of respectively the undpoed DNP matrix and the DNP matrix containing the radical in presence of microwave irradiation.

S5 Error estimation for the NMR experiments

The estimation of errors of the enhancements and of the contribution factor were done according to Lelli et al[15]:

$$\Delta\varepsilon = \varepsilon \left(\frac{\Delta I_{\text{on}}}{I_{\text{on}}} + \frac{\Delta I_{\text{off}}}{I_{\text{off}}} \right) \qquad (3)$$

$$\Delta\theta = \theta \left(\frac{\Delta I_{with\ radical}}{I_{with\ radical}} + \frac{\Delta I_{without\ radical}}{I_{without\ radical}} \right) \qquad (4)$$

were ΔI is the error of the observed signal with an integral of I with and without μw, or in the case of the contribution factor, the signal intensity in a solution with or without radical. The relative errors are generally higher in spectra recorded without μw. The absolute errors are generally higher with higher enhancement factors. We reported the highest absolute error as the error bar for each curve, even if this procedure overestimates the errors of the single points.

A manual baseline correction was applied in spectra recorded at 800 MHz, as probe background signals could not be completely suppressed. The manual baseline correction can introduce an additional error especially for broad peaks with unresolved side band patterns at low spinning speeds. The reproducibility of the baseline correction was tested by repeating the procedure three times on the same spectra and recording the variation of the results. Taking into account the sum of both error sources, an error bar of 5 % of the highest enhancement in each data series and of 10 % of the highest contribution factor in each series was applied, even if this procedure may overestimate the error of the single points.

To estimate the error of the TB,OFF and TB,ON measurements, the polarization build up curves were fitted with monoexponential curves. The biggest error of the fit was found to be ± 4 % of TB,OFF. This value was applied to all data series, even if this procedure overestimates the errors of some points.

S6 EPR Experiments

S6.1 Experimental conditions.

Low-temperature W-band EPR measurements were carried out on a Bruker E680 spectrometer at a μw frequency of 94 GHz and a temperature of 100 K, on 0.1 mM frozen solutions of the binitroxide radicals in glycerol-d_8/D_2O/H_2O (6/3/1 v%). $\pi/2$ and π pulses of 52 and 104 ns were used, respectively. EPR spectra were recorded using field-dependent echo detection (echo-detected EPR). Longitudinal relaxation (T_{ir}) times were recorded with the inversion recovery sequence, and transverse relaxation (T_m) times were recorded using a variable delay Hahn echo sequence. The Hahn echo delay time for the inversion recovery detection and the initial echo delay in the transverse relaxation measurements was set to 400 ns. The data were fitted with a stretched exponential to account for a distribution of the values. The first moment of this distribution is indicated as the mean value (as described below). The relaxation curves were recorded at the EPR intensity maxima of the BDPA and nitroxide moieties. Solution-state X-band (9.4 GHz) continuous-wave (CW) EPR measurements were carried out on Bruker EMX nano at 295 K with 1 mM solutions of the free radicals in glycerol-d_8/D_2O/H_2O (6/3/1 v%). All EPR spectrum simulations were performed using the EasySpin EPR simulation package for MATLAB.

S6.2 Electronic relaxation constants

In analogy to Zagdoun *et al.*,[16] the longitudinal electronic relaxation time traces were fitted using a stretched exponential function:

$$I(t) = I_0 + I_1 \cdot e^{-\left(\frac{t}{T^*_{1e}}\right)^{\beta}} \qquad (5)$$

where I_0 is the initial intensity, I_1 the proportionality factor, T^*_{1e} the decay time parameter and β the stretching parameter. The mean relaxation time is given as the first moment $<T_{1e}>$ of the distribution as a mean, called the inversion recovery time T_{ir}:

$$T_{ir} = \langle T_{1e} \rangle = \int_0^{\infty} e^{-\left(\frac{t}{T^*_{1e}}\right)^{\beta}} dt = \frac{T^*_{1e}}{\beta} \Gamma\left(\frac{1}{\beta}\right) \qquad (6)$$

The transverse electronic relaxation times were recorded using a variable delay Hahn echo sequence and fitted with a stretched exponential.

$$I(t) = I_0 \cdot e^{-\left(\frac{t}{T^*_{2e}}\right)^{\beta}} \qquad (7)$$

S23

where I_0 is the initial intensity, T^*_{2e} the decay time parameter and β the stretching parameter. The mean transverse relaxation time is given as the first moment $\langle T_{2e}\rangle$ of the distribution as a mean, called the phase memory time T_m:

$$T_m = \langle T_{2e}\rangle = \int_0^\infty e^{-\left(\frac{t}{T^*_{2e}}\right)^\beta} dt = \frac{T^*_{2e}}{\beta}\,\Gamma\left(\frac{1}{\beta}\right) \qquad (8)$$

S6.3   Error estimation of T_{ir} and T_m

To estimate the error of the electronic relaxation times T_{ir} and T_m, the confidence intervals (95 %) of the fit for the relaxation time constants and the stretching parameter β were added. The sum of both confidence intervals was below 0.1 ms for T_{ir} and below 0.1 µs for T_m, consequently, 0.1 ms or 0.1 µs, respectively, were indicated as upper limits.
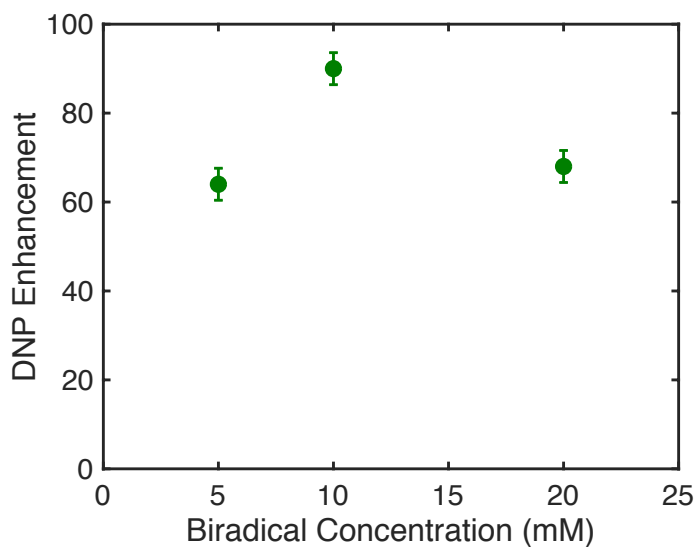
S7 Supplementary figures

Figure S15. Proton enhancement of M-TinyPol at different biradical concentration in d_8-glycerol/D_2O/H_2O 60/30/10 (v/v/v). The enhancements were measured at 18.8 T and 110 K sample temperature, with a MAS rate of 40 kHz.
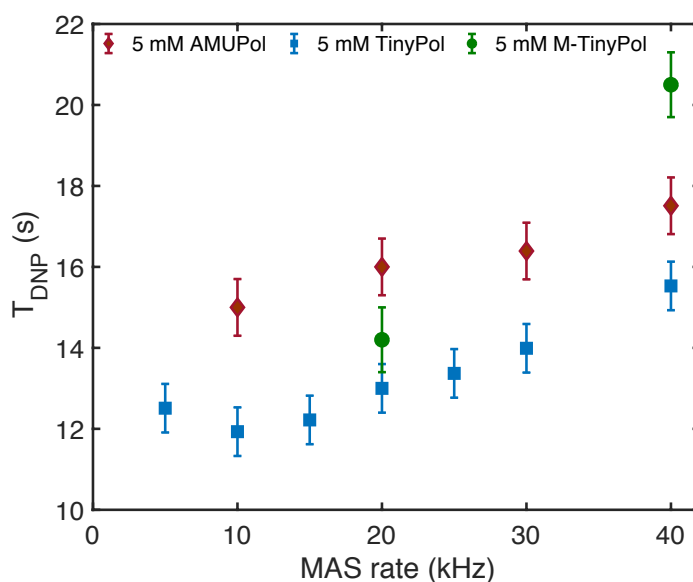

Figure S16. DNP build up times (T_{DNP}) measured in the presence of microwave irradiation for 5 mM TinyPol, M-TinyPol, and AMUPol in d_8-glycerol/D_2O/H_2O 60/30/10 (v/v/v) as a function of the spinning frequency. These build-up times were measured at 18.8 T and 110 K sample temperature.
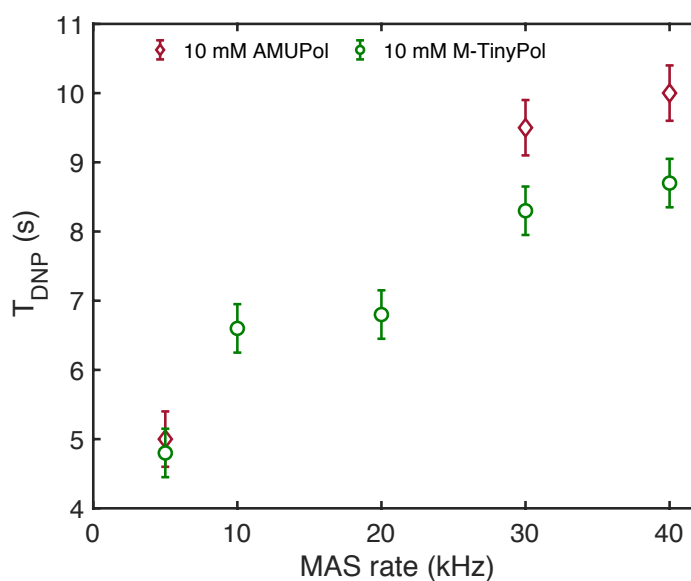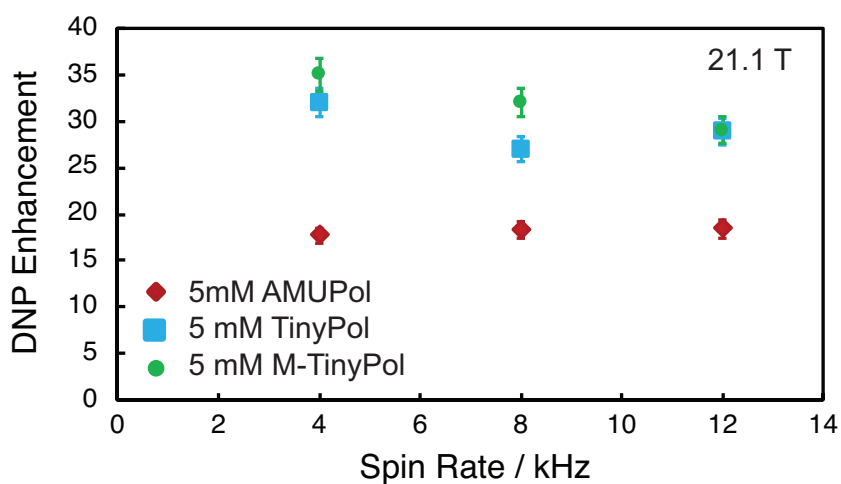
Figure S17. DNP build up times (T_{DNP}) measured in the presence of microwave irradiation for 10 mM TinyPol, M-TinyPol, and AMUPol in d_8-glycerol/D_2O/H_2O 60/30/10 (v/v/v) as a function of the spinning frequency. These build-up times were measured at 18.8 T and 110 K sample temperature.

Figure S18. MAS frequency dependence of the DNP enhancements for 5 mM AMUPol, TinyPol and M-TinyPol in d_8-glycerol/D_2O/H_2O 60/30/10 (v/v/v), measured at 21.1 T in 3.2 mm rotors on the carbon-13 resonances of proline from CPMAS experiments. A sample temperature of 115 K ± 7 K was maintained over the whole spinning range for microwave on experiments and of 90 K ± 5 K for microwave off experiments. The reported enhancements correspond to the mean value of the enhancement factors measured on the five ^{13}C resonances of proline.
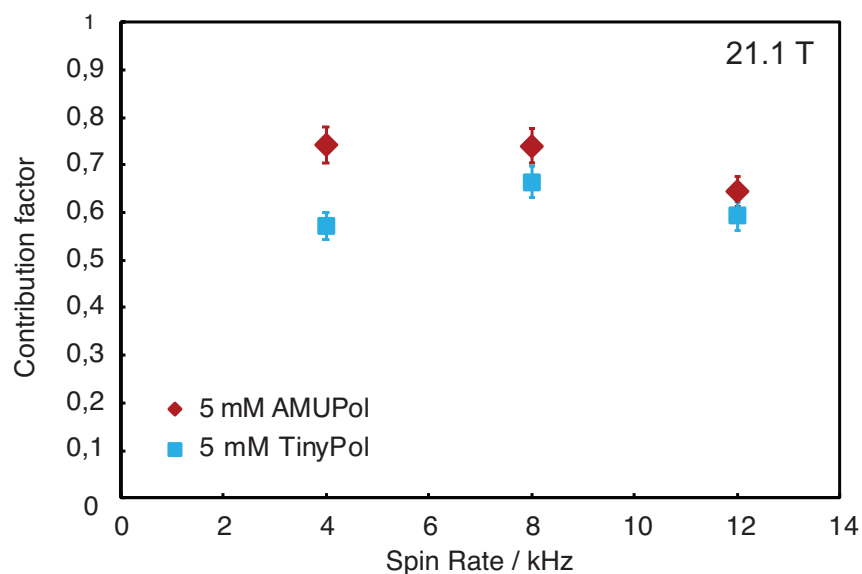
Figure S19. MAS frequency dependence of the contribution factor measured for 5 mM AMUPol and TinyPol in d_8-glycerol/D_2O/H_2O 60/30/10 (v/v/v) at 21.1 T, estimated from the ^{13}C resonances of proline in CPMAS experiments.
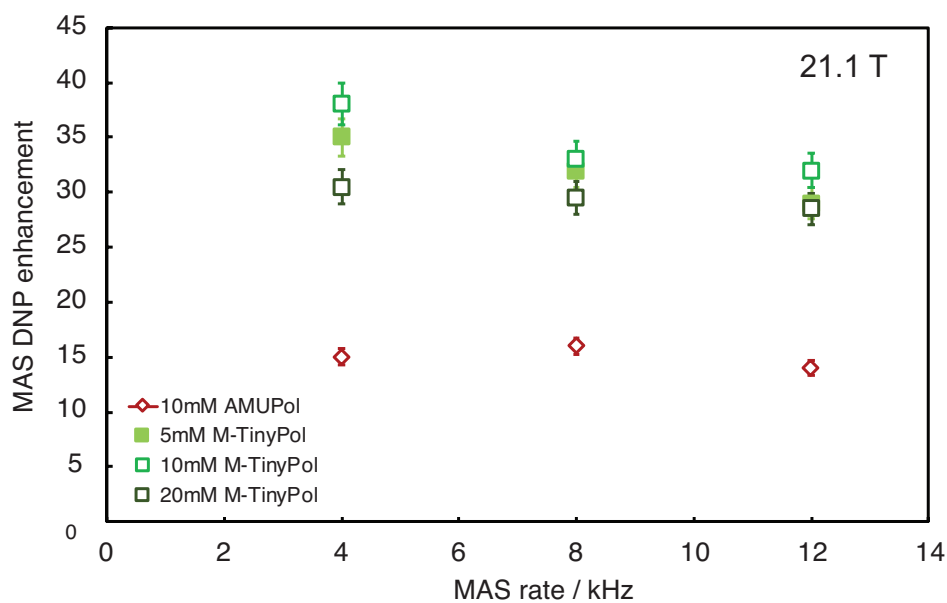

Figure S20. MAS frequency dependence of the DNP enhancements for various concentrations of M-TinyPol and 10 mM AMUPol in d_8-glycerol/D_2O/H_2O 60/30/10 (v/v/v), measured at 21.1 T in 3.2 mm rotors on the ^{13}C resonances of proline from CPMAS experiments.
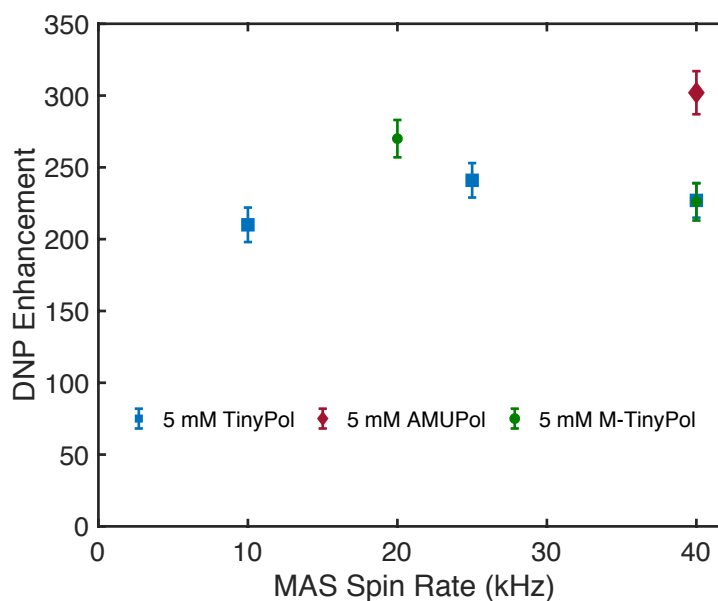
Figure S21. MAS frequency dependence of the DNP enhancements for 5 mM AMUPol, TinyPol and M-TinyPol in d_8-glycerol/D_2O/H_2O 60/30/10 (v/v/v), measured at 9.4 T in 1.3 mm zirconia rotor. A sample temperature of 110 K ± 5 K was maintained over the whole spinning range.
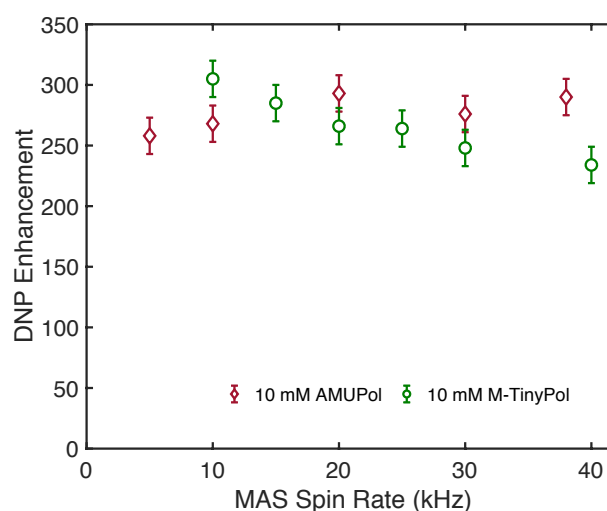

Figure S22. MAS frequency dependence of the DNP enhancements for 10 mM AMUPol and M-TinyPol in d_8-glycerol/D_2O/H_2O 60/30/10 (v/v/v), measured at 9.4 T in 1.3 mm

zirconia rotor. A sample temperature of 110 K ± 5 K was maintained over the whole spinning range.
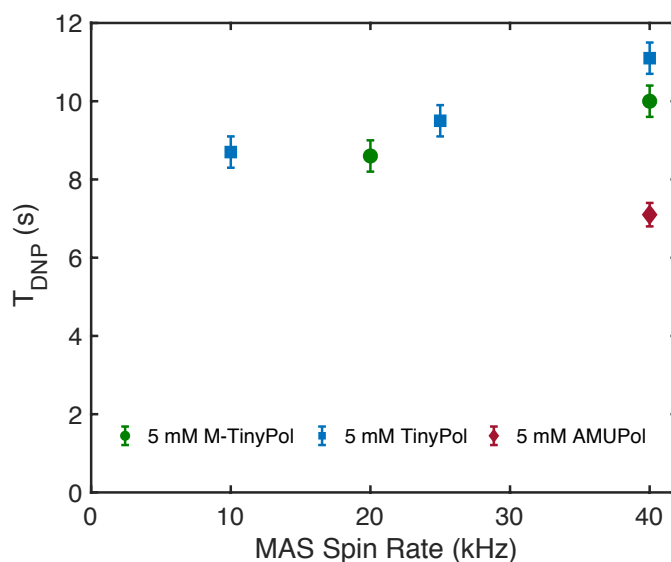

Figure S23. DNP build up times (T_{DNP}) measured in the presence of microwave irradiation for 5 mM TinyPol, M-TinyPol, and AMUPol in d_8-glycerol/D_2O/H_2O 60/30/10 (v/v/v), as a function of the spinning frequency. These build-up times were measured at 9.4 T and 110 K sample temperature.

Figure S24. DNP build up times (T_{DNP}) measured in the presence of microwave irradiation for 10 mM M-TinyPol and AMUPol in d_8-glycerol/D_2O/H_2O 60/30/10 (v/v/v) as a function of the spinning frequency. These build-up times were measured at 9.4 T and 110 K sample temperature.
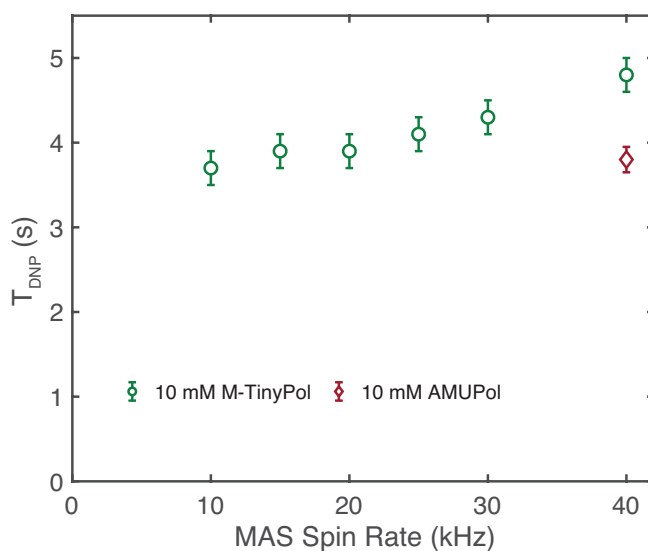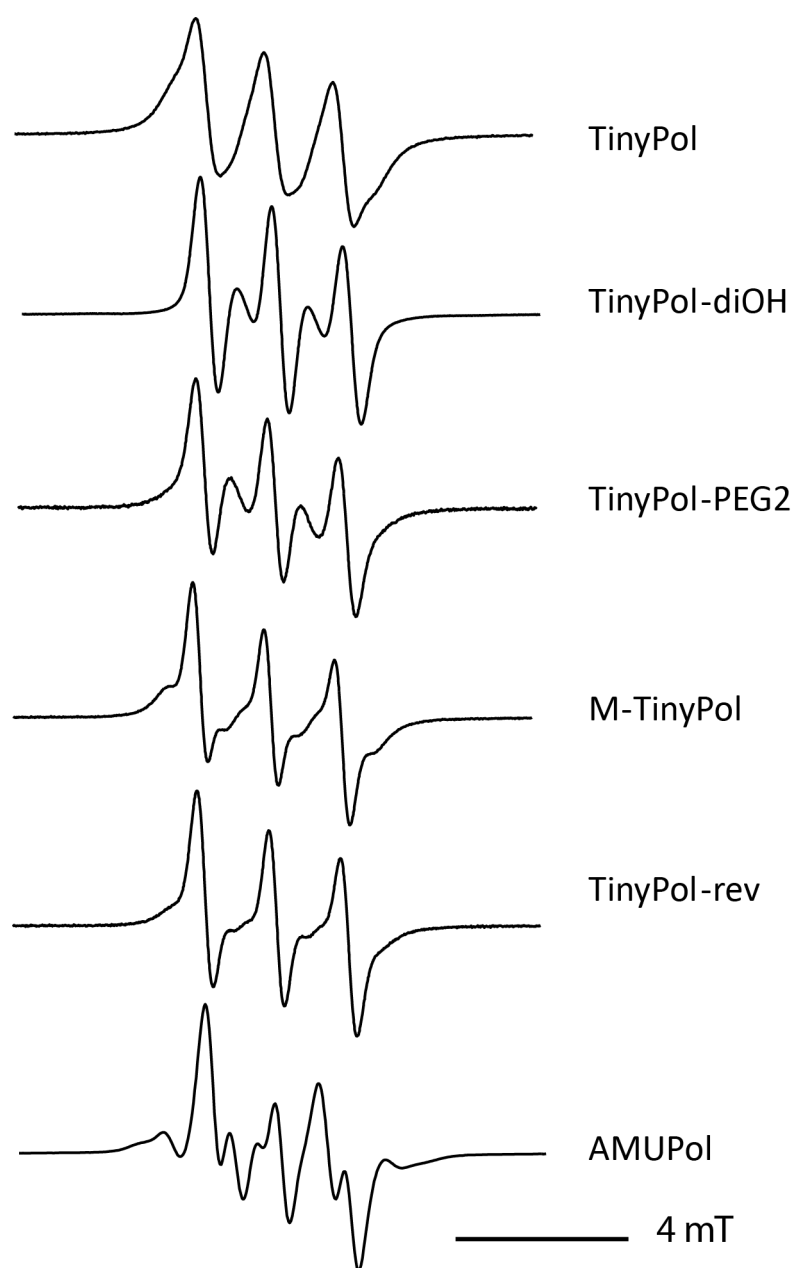
S29

TinyPol

TinyPol-diOH

TinyPol-PEG2

M-TinyPol

TinyPol-rev

AMUPol

4 mT

Figure S25: X-band CW EPR of 0.1 mM radicals in water at room temperature.
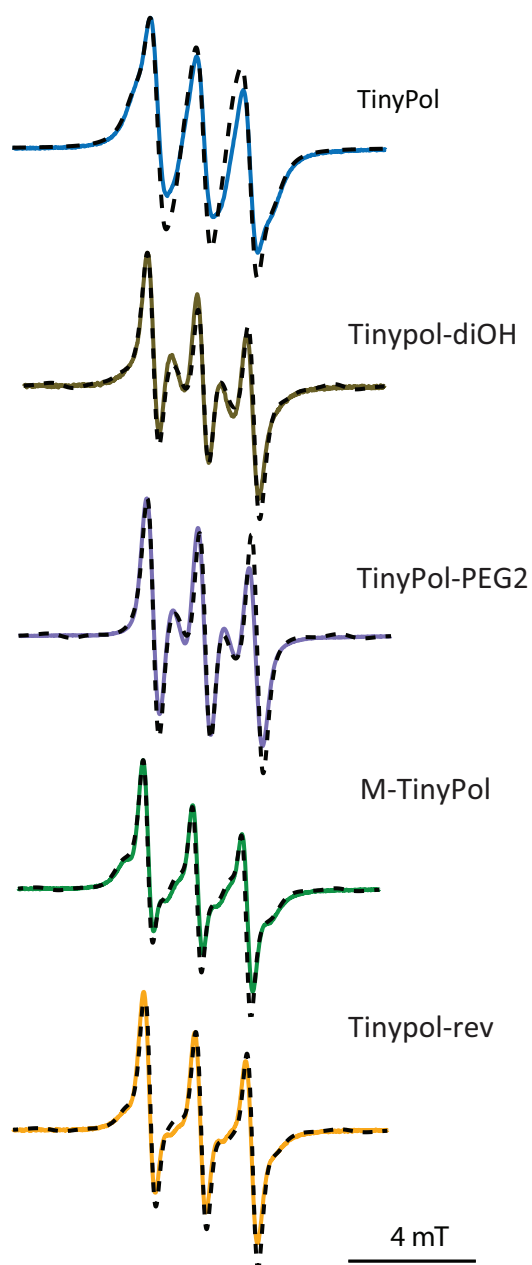
Figure S26: Experimental data (in color) and fits (in black dotted lines) of TinyPols X-band EPR spectra in water. The data were fit using the Matlab package EasySpin. The fitting was performed with the "pepper" function, though it is originally intended to be used in solid state, in order to speed up the calculations without losing accuracy in this case, as explained in Tagami et al. (17). The initial g, A, and J coupling values were set to those found for AMUPol by Soetbeer et al (18). The use of a multicomponent fit was rationalized with the bimodal distribution found in the MD simulations of TinyPol shown in Figure S9. The best fit was found using the 3 different isotropic J components and adding a gaussian line broadening width of 10-15 MHz for each component. The extracted J values are reported in Table S1.

	J-coupling (MHz) (weight %)
TinyPol	<5 (23%) 24 (47%) 110 (30%)
M-TinyPol	<5 (12%) 28 (44 %) 122 (44 %)
TinyPol-diOH	<5 (18%) 30 (30%) 112 (52%)
TinyPol-PEG2	<5 (37%) 30 (0%) 112 (63%)
TinyPol-rev	<5 (22%) 29 (32%) 117 (45%)

Table S1: Isotropic *J* coupling values and relative weight obtained by fitting the EPR spectra of Figure S21.
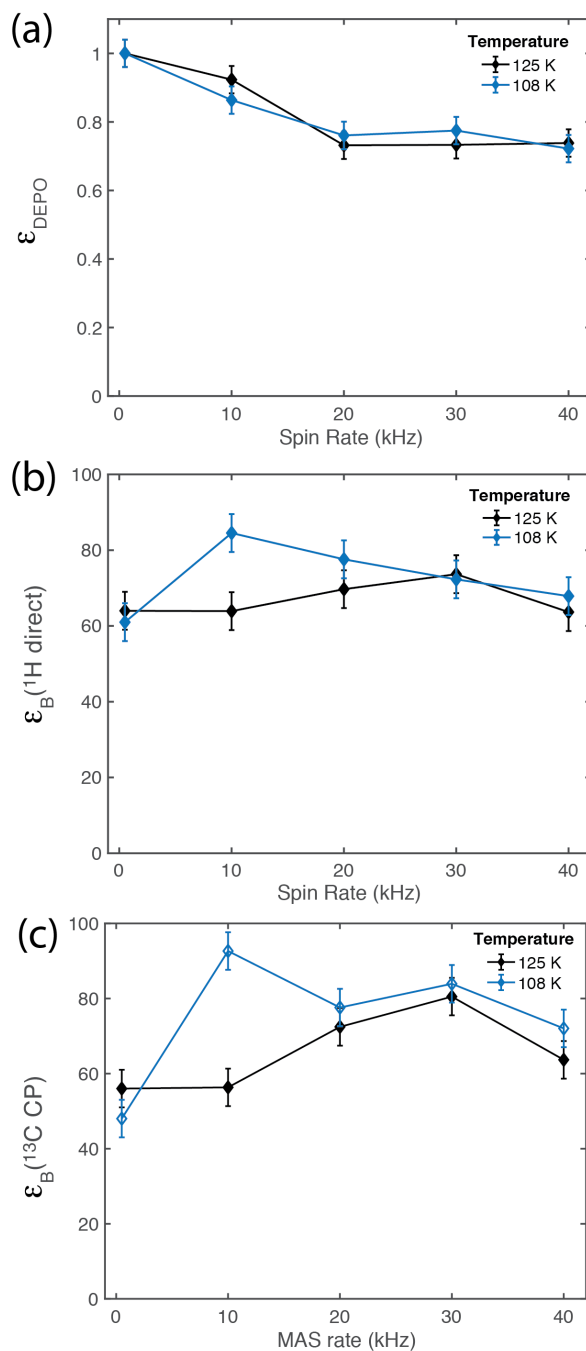
Figure S27. MAS frequency dependence of (a) ε_{depo} and (b) $^{1H}\varepsilon_B$ direct calculated from $\varepsilon_{On/off}$ (direct 1H) $*\varepsilon_{depo}$ and (c) $^{1H}\varepsilon_B$ determined from the 1H enhancement estimated on 13C via 1H-13C CP multiplied by ε_{depo}, as reported in Fig 2b from ref 19, measured on 2 M ^{13}C-urea in a 5 mM TinyPol in (6: 3:1 v%) d8-glycerol:D2O:H2O solution ,in a 1.3 mm rotor at 18.8 T, under two temperature conditions. These measurements were performed in order to demonstrate that, under the exact same experimental conditions as those described for the AsymPolPOK radical (ref), TinyPol clearly outperforms the latter, leading to a substantial improvement in DNP performance at high magnetic field and fast spin rate. ε_{depo} was obtained as the ratio of the signal intensity at the given spin rate and the signal intensity at 0 kHz spin rate with a recycle delay of 5* $T_{B,off}$ in the absence of microwave irradiation ; $\varepsilon_B = \varepsilon_{On/Off} * \varepsilon_{depo}$.
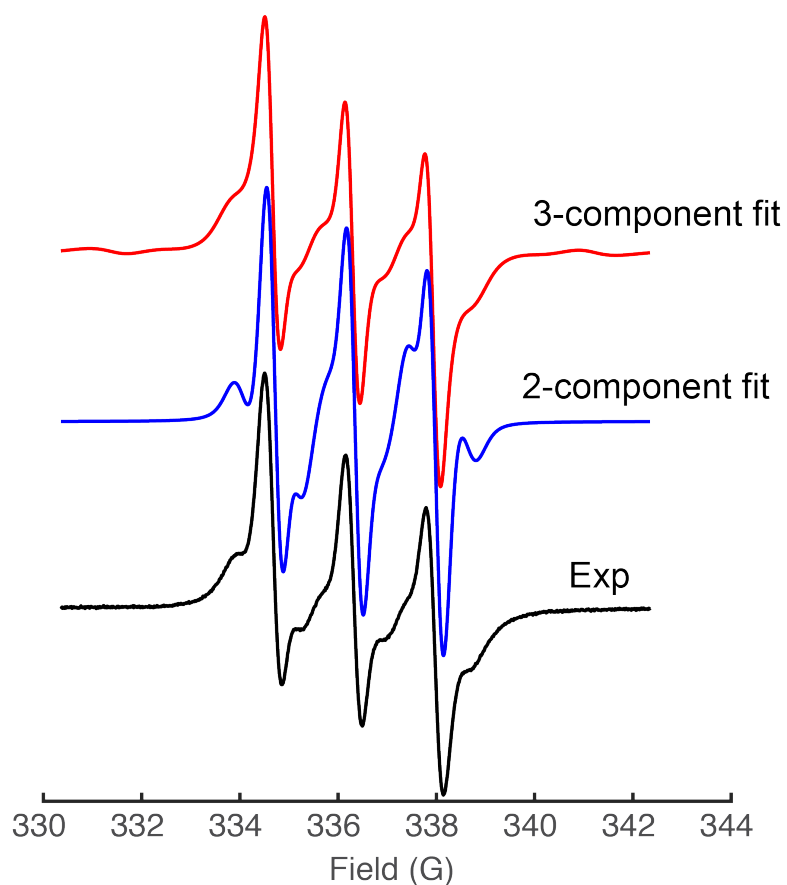
Figure S28: Experimental X-band EPR spectrum in water of M-TinyPol (in black) and fits using 2 (in blue) or 3 (in red) components. In the 2-component fit, values of J=0 MHz (17%) and J=28 MHz (83%) were obtained. In the 3-component fit, values of J=0 MHz (12%), J=28 MHz (44%) and J=122 MHz (44%) were obtained. Adding a larger J coupling value allows a more accurate fit of the experimental data. The interpretation of the fit should however be taken with caution and the fitting is just meant to illustrate the wide span of the J coupling distribution in TinyPols.

S8 References

1. K. Sakai, K. Yamada, T. Yamasaki, Y. Kinoshit, F. Mito and H. Utsumi, *Tetrahedron* 2010, **66,** 2311-2315.
2. D. J. Kubicki, G. Casano, M. Schwarzwälder, S. Abel, C. Sauvée, K. Ganesan, M. Yulikov, A. J. Rossini, G. Jeschke, C. Copéret, A. Lesage, P. Tordo, O. Ouari and L. Emsley, *Chem. Sci.* 2016, **7,** 550-558.
3. E. J. Rauckman, G. M. Rosen and M. B. Aboudonia *J. Org. Chem.* 1976, **41,** 564 -565.
4. C. Sauvée, M. Rosay, G. Casano, F. Aussenac, O. Ouari and P. Tordo, *Angew. Chem. Int. Ed. Engl.* 2013, **52,** 10858-10861.
5. M. J. Abraham, T. Murtola, R. Schulz, S. Páll, J. C. Smith, B. Hess and E. Lindahl, *SoftwareX* 2015, **1,** 19-25.
6. V. Hornak, R. Abel, A. Okur, B. Strockbine, A. Roitberg and Simmerling, *PROTEINS: Structure, Function, and Bioinformatics* 2006, **65,** 712-725.
7. E. Stendardo, A. Pedone, P. Cimino, M. C. Menziani, O. Crescenzi and V. Barone, *Phys. Chem. Chem. Phys.* 2010, **12,** 11697-11709.
8. M. J. Frisch, G. W. Trucks, H. B. Schlegel, G. E. Scuseria, M. A. Robb, J. R. Cheeseman, G. Scalmani, V. Barone, G. A. Petersson, H. Nakatsuji, M. C. X. Li, A. V. Marenich, J. Bloino, B. G. Janesko, R. Gomperts, B. Mennucci, H. P. Hratchian, J. V. Ortiz, A. F. Izmaylov, J. L. Sonnenberg, D. Williams-Young, F. Ding, F. Lipparini, F. Egidi, J. Goings, B. Peng, A. Petrone, T. Henderson, D. Ranasinghe, V. G. Zakrzewski, J. Gao, N. Rega, G. Zheng, W. Liang, M. Hada, M. Ehara, K. Toyota, R. Fukuda, J. Hasegawa, M. Ishida, T. Nakajima, Y. Honda, O. Kitao, H. Nakai, T. Vreven, K. Throssell, J. A. Montgomery, J. E. P. Jr., F. Ogliaro, M. J. Bearpark, J. J. Heyd, E. N. Brothers, K. N. Kudin, V. N. Staroverov, T. A. Keith, R. Kobayashi, J. Normand, K. Raghavachari, A. P. Rendell, J. C. Burant, S. S. Iyengar, J. Tomasi, M. Cossi, J. M. Millam, M. Klene, C. Adamo, R. Cammi, J. W. Ochterski, R. L. Martin, K. Morokuma, O. Farkas, J. B. Foresman and D. J. Fox *Gaussian 16, Revision A.03,* Wallingford CT, 2016.
9. K. Yamaguchi, H. Fukui and T. Fueno, *Chem. Lett.* 1986, **15,** 625-628.
10. K. R. Thurber and R. Tycko, *J. Magn. Reson.* 2009, **196,** 84−87.
11. I. Romanenko, D. Gajan, R. Sayah, D. Crozet, E. Jeanneau, C. Lucas, L. Leroux, L. Veyre, A. Lesage, L. Emsley, E. Lacote and C. Thieuleux, *Angew. Chem. Int. Ed.* 2015, **54,** 12937-12941.
12. R. Bendall, M. and R. E. Gordon, *J. Magn. Reson.* 1983, **53,** 365.
13. M. R. Bendall and D. T. Pegg, *Magn. Reson. Med.* 1985, **2,** 91.
14. D. G. Cory and W. M. Ritchey, *J. Magn. Reson.* 1988, **80,** 128.
15. M. Lelli, S. R. Chaudhari, D. Gajan, G. Casano, A. J. Rossini, O. Ouari, P. Tordo, A. Lesage and L. Emsley, *J. Am. Chem. Soc.* 2015, **137,** 14558-14561.
16. A. Zagdoun, G. Casano, O. Ouari, M. Schwaerzwalder, A. J. Rossini, F. Aussenac, M. Yulikov, G. Jeschke, C. Copéret, A. Lesage, P. Tordo and L. Emsley, *J. Am. Chem. Soc.* 2013, **135,** 12790-12797.
17 Tagami, K.; Equbal, A.; Kaminker, I.; Kirtman, B.; Han, S. Solid State Nuclear Magnetic Resonance. Solid State Nucl. 2019, **101**, 12–20.
18 Soetbeer, J.; Gast, P.; Walish, J. J.; Zhao, Y.; George, C.; Yang, C.; Swager, T. M.; Griffin, R. G.; Mathies, G. Phys. Chem. Chem. Phys. 2018, **20** (39), 25506–25517.
19. Mentink-Vigier, F.; Marin-Montesinos, I.; Jagtap, A. P.; Halbritter, T.; van Tol, J.; Hediger, S.; Lee, D.; Sigurdsson, S. T.; De Paepe, *J. Am. Chem. Soc.* 2018, **140** (35), 11013–11019.